Proceedings of the Eighth International Symposium on ECHE, 1984, Dubrovnik

INTELLIGENT MOVEMENT MEASUREMENT DEVICES

E. H. Furnee, Delft, the Netherlands
Prosthetic Control Lab, Dept. of
Applied Physics, Univ. of Technology

VIDEO CONVERTER WITH REAL-TIME MARKER PROCESSOR

For human movement studies by opto-electronic recording the author has applied television cameras and developed video-to--digital conversion systems as early as reported in (Furnee, 1967). Follow-up on the original design has been reported in (Paul and Jarrett, 1974) and (Jarrett, 1976) from the U.K. Strathclyde University and Dundee Limb Fitting Centre. The latter system has been commercially adopted and improved as VICON by Oxford Medical Computers. Similar developments in the U.S.A. have been documented in Ph.D. theses (1969) and reported in (Dinn and Winter, 1970) up to the recent United Technologies system in (Taylor e.a., 1982).

Common to these systems are television cameras viewing contrasting landmarks attached to the subject, and a video-to-digital converter digitizing the x,y coordinates of landmark points in the tv image. The essential process is a digital counting operation: counting and readout of tv-line number for vertical position, and for horizontal position high-speed counting and readout of time increments during the tv-line scan. The tv-lines are of near enough constant duration in a quality camera, or made to be constant by digital synthesis of deflection voltages. Counter readout is strobed upon detecting the markers by threshold crossing of video signal (fig. 1).

These tv-based marker detection systems thus automatically generate the digital position codes which are fed into computers for further processing. Important common requirement is a

software tracking module for identifying the landmarks, as the coordinate codes are generated in an ordering by vertical values, which only in simplest gait studies may coincide with landmark numbering. Various authors have furthermore reported software for 3-D reconstruction of landmark positions as seen from two or more sensors, which finds application in the present systems (Woltring, 1975, 1980; Whittle, 1982; Cappozzo, 1983).

The landmark points as seen by the camera are in all present converters restricted to circumference points or contours, as defined by black-white-black transitions on each tv-line intersection, skipping all interior points.

The systems from the author's Prosthetic Control Laboratory have always included some intelligent hardware, allowing further selective suppression of landmarpoints before digitizing. This option in limiting the data flow into the computer, unburdening the often slow or crowded transmission and storage media (fig. 2).

Previous versions allowed the automatic selection on each marker contour of one or two pairs of points, sufficiently far apart on opposite sides of the center. Special hardware inhibits the counter readout strobe for all other points. From this much reduced data the computer calculates the centroid's estimated coordinates to represent each marker's position. For greater precision one selects the complete contour output, and follows Winter's method of centroid estimation, if sufficient on-line computing facilities are available.

As a logical step of incorporating programmable intelligence into the measuring device, this presentation describes the newest video--to-digital position encoder with built-in microprocessor system.

This performs in each tv-frame of 1/60 second the real-time computation of up to 20 markers' centroids from the complete contours (fig. 3, fig. 4).

Finally, the output data of the instrument is just what we want to measure: the running markers positions, a single pair of coordinates for each marker, with resolutions of 1:4000 in x and y. Optionally, additional output are marker sizes in the horizontal and vertical sense, for monitoring or discrimination purposes.

This reduction to essential data allows further convenient processing of trajectories, angles, speeds etc. on less massive computing facilities which become ever more available to the clinical investigator. Intelligent measurement devices promote independence in time and place for the planning of routine and critical experiments in the life sciences.

Innovative features will be discussed, such as uniform field of view illumination by specially directed LED-rings around the camera objective.

POSITION-SENSITIVE PHOTOCELL WITH MULTI-FREQUENCY SYNCHRONOUS DETECTOR

Introduction

Opto-electronic movement recording with higher samplerates than obtainable with normal tv-cameras has been reported in (Lindholm & Oeberg, 1974). In contrast with tv they applied a non-scanned sensor consisting of a planar homogeneous silicon cell with four side electrodes as described in (Wallmark, 1957). Using lateral photo-effect, this high-speed sensor allows to determine the centre of gravity of radiation imaged on the several cm square surface, as indicated in fig. 5.

The movement analysis application, which led to the commercial development of the Selspot system by Selcom AB, Sweden, requires the attachment of active radiation sources as landmarks to the subject, in the form of light emitting diodes (LED´s) with concomitant wiring.

A brief description of Selspot features is needed before introducing what is believed to be an improved development from the authors Prosthetic Control Laboratory, from the point of view of ambient light and reflection error susceptibilities.

Sequential pulse activation of the Selspot LED´s allows separate pulse amplitude measurements for each landmark LED, so the landmarks are easily identified by time-multiplex (tv-systems as described above require software tracking for landmark identification).

The use of short-duration pulses implies a high signal bandwidth,

extending form dc (0 hz) to the order of 20 kHz. The measurement principle gives no scope for bandwidth reduction, so the sensor and associated electronics noise retains the same high bandwidth. The signal-to-noise ratio, however, benefits from the high light pulse intensities, such that in the best circumstances the random error is specified as + or - 0,03 % nominal of measuring range, only slightly above the specified resolution of 1:4.000 (Selspot II).

The Selspot II scan-rate is 10.000 measurements per second, divided by the number of LED´s, only to be sustained for 2 seconds followed by 30 seconds LED´s off. Continuous measurement is specified at 1:8 of the above rate, e.g. 208 measurements per second for 6 LED´s.

Infrared LED´s and infrared filtering in front of the sensor is a Selspot requirement for reducing position errors by ambient and background lights projected on the sensor, against which the centre-of-gravity measurement principle cannot discriminate. The assumption that ambient light is limited to the visible spectrum not being always met, the newer version Selspot II has a further active ambient error reduction scheme. Here, according to trade litterature, the LED light intensity is for each sample adaptively increased until it surpasses by a preset factor the ambient intensity value as monitored between samples. No numerical specifications are given for this ambient light suppression capability, which is seen to be a relative error reduction and no cancellation.

The Selspot requirement of infrared LED´s for ambient light suppression entails a serious error source reported in (Gustafsson & Lanshammar, 1977), infrared radiation being prone to reflection on almost all, even non-specular surfaces. This gives rise to spurious pathways and false images on the sensor surface, shifting the centre of gravity and thus the measured position away from the direct LED image. The cited authors report vertical reflection error over a concrete floor of up to 10 cm in a 160 cm high and 270 cm wide field of view. By calibrating a least-squares polynomial fit to 21 LED locations and evaluating this compensation with 35 LED positions these authors found the expected coordinate error reduced by approximately a factor 2,5, the maximum values being

about 4 times reduced. Remaining errors appear thus in the order of 1 % or 40 times the specified resolution. These trials were without ceiling and walls influence and without the self-reflections of an actual human subject. Quite different from most other instrumentations, the reflection problem calls for fine grid calibration, not once for non-linearities of the instrument itself, but repeatedly for every change of the measuring environment as this influences the measurements in a non-linear and unpredic--table way.

SYNCHRONOUS DETECTION SYSTEM

Based on the same or similar position-sensitive photocell, the author's Prosthetic Control Laboratory has developed a LED activation and detection system with inherent ambient and background light suppression. This permits the use of visible LED light so as to eliminate the problem of spurious reflections. This system takes care of two main Selspot error sources, by introducing continuous sinusoid LED light waveforms and applying the methods of synchronous detection (principle in fig. 6, multi-LED sampled--data fig. 7).

In synchronous detection systems, the unknown amplitude of a sinusoid received signal with certain frequency is measured through multiplication with a sinusoid detector signal of the same frequency, and determining the product's average value over an integer number of periods (more imprecisely, a low-pass filter can follow the multiplier). In formulas:

received signal	$r(t) = a \sin(2 \pi f t + psi)$
detector, or coherent signal	$c(t) = 2c \sin(2 \pi f t)$
product	$p(t) = a \cdot c \cos psi - a \cdot c \cos(4 \pi f t + psi)$
average, or sumproduct	$p = a \cdot c \cos psi$ constitutes a measurement of a.

The measurement interval I = m/f, the measurement rate M = f/m, m integer (1). In communication systems like single-sideband receivers, the phase psi is usually unknown. In a measurement system, the transmitted signal is self-provided such to maintain cos psi=1.

A dc component in the received signal d(t) = d gives the product cd sin(2pi ft) whose average over I is zero. This feature eliminates

such ambient or back-ground light as is constant per interval I: daylight, 90% of incandescent light, or 60% of fluorescent light.

Any frequency component different from the detector frequency f, as represented by

$$r'(t) = a'\sin(2\pi f't + phi),$$ results in a product

$$p'(t) = a'c\cos(2\pi (f'-f)t + phi) - a'c\cos(2\pi (f'+f)t + phi) \quad (2)$$

whose average over interval I

$$P(f',phi) = 0 \text{ for any frequency } f' = m'M, \; m' \text{ integer unequal } m, \text{ any phi} \quad (3)$$

For frequency components f' other than integer multiples of the measurement rate, the average of (2) leads to an expression with terms like $\cos(k'x + phi)\sin(kx) / \sin x$, $k' = k-e$, e small, x involving f'-f or f'+f. (4)

This average product function P(f',phi) pictured in fig. 8, has a narrow main maximum centered at f' = f and decreasing sidelobes extending both ways. The zeros interventing between the main and sidelobes are given by (3), and depending on the value of phase phi, there is another series of equidistant zeros, intermediate or coinciding with (3).

The synchronous detector action is thus equivalent to a narrow bandfilter centered at the coherent frequency f, with bandwidth and zero positions depending on the measurement rate M. The frequency-dependent transfer function may also be viewed as the Fourier transform of the rectangular window implied by the observation and summation interval I.

A bandfilter of rectangular shape, centered at frequency f and passing the same amount of power as the main lobe and all sidelobes, provides a convenient measure of the synchronous detector's bandwidth, fig. 9. This so-called equivalent noise bandwidth (Harris, 1978) turns out to be half the measuring rate,

$$ENWB = M/2 \text{ (Hz)}, \text{ regardless of phase phi} \quad (5)$$

As a numerical example, the measuring rate M = 212 Hz, the coherent LED-frequency f = 8480 Hz and the synchronous detector acts like a

sharp bandfilter with ENWB = 106 Hz.

The attenuation of the synchronous detector transfer function for low frequencies, like 100 Hz, the dominant ripple frequency of incandescent or fluorescent ambient or background light, is in this example better than a factor 50, for worst-case phi. With eight times higher LED-frequencies, still well below the below--mentioned systems´ sample rate, this attenuation factor becomes 400. The LED-signals not being pulses but sinusoids with signle frequencies above 5 kHz, the synchronous detector system allows pre-filtering for further attenuating any low-frequency ambient light ripple, say by 48 db over 4 octaves, or a factor of 250. Total ripple rejection can thus be better than 1:100.000, while dc rejection is absolute.

For a multi-marker system as required by movement analysis as many LED´s are applied, which calls for a multi-frequency synchronous detector system. The equations (3) show that for any LED- and coherent frequency fi = mi M, the synchronous detector output is zero for any other frequency fj = mj M, j unequal i.

Thus by a proper choice of LED-frequencies as a range of integer multiples of the measurement rate, synchronous detection allows continuous and simultaneous measurement of multiple LED´s, as it were in frequency-multiplex. The system can thus be viewed as a Fourier analyzer for a limited number of fixed frequencies. This leads to the observation that any influence of phase phi could be eliminated by adding cosine-multiplication and further processing.

As an extension to the numerical example, six adjacent LED-frequencies are: 5088, 6360, 6996, 8480, 9328 and 11660 Hz.

These frequencies, multiples of the measurement rate of 212 Hz, have been chosen so that their harmonics do not coincide with any of the fundamentals. This eliminates as a possible error source any non-linearities, most notable in the high-energy LED-characteristics.

By proper choice of the LED-signal phases, the peak values of the sumsignal impinging on the sensor can be restricted within bounds expressed by the crest-factor.

In the numerical example, the crest-factor for equal LED-amplitudes could be minimized to a value of 1,66 (relative to peak-value of a pure sine having the same root-mean--square value as the sumsignal). A crest margin for the case of unequal LED-signal amplitudes implies a practical limit to the applicable number of LED´s and a need for wide-range or high--resolution a/d converters.

As the narrow-band characteristic of synchronous detection implies up to 200 times less noise bandwidth than Selspot systems, the sensor and pre-amplifier noise is effectively reduced. This performance is partly offset by LED temperature considerations, imposing lower amplitudes in continuous sinusoids than allowed with pulse operation. Also red LED efficiency is lower than with existing infrared types. The prototype at Prosthetics Control Laboratory (Oostinjen, 1982) shows a r.m.s. noise error of 1:4.000. This measure of meaningful resolution compares well with Selspot II, though the synchronous detector outputs code encompasses more than the equivalent 12 binary bits.

The prototype multi-frequency synchronous detector makes full use of sampled-data digital signal processing electronics, fig. 7. The LED-and detection sinusoids are generated from read-only--memory (EPROM). To extend the numerical example, the systems sample rate is 279.840 steps per second, organized as 212 cycles of 1320 samples. At this rate of ca 3,5 microsecond per step, the LED and coherent signals are renewed, and sensor outputs are sampled and converted to digital code. Parallel banks of LSI serial-parallel multipliers with accumulators provide the sumproducts over each cycle, for each LED and each of the four sensor channels. This organisation requires no additional random-access-memory (RAM), but will be replaced by fast RAM plus a reduced number of fast fully parallel multipliers and a microcomputer to process each cycle as to sensor channel subtraction and division providing the position coordinates.

DISCUSSION

Only a few laboratories and investigators are in a position to advance formal methodology and contribute to the formulation of concepts and answering of relevant questions in human movement strategy and clinical gait evaluation (Cappozzo, 1983). Although the cited author reports a satisfying state of the art with instrumentation hardware, to which he has himself contributed, such research centers can be expected to further profit from improved accuracy, dependability and applicability of measurement devices in the not too heavily instrumented clinical environment.

For human movement recording, we have presented a television conversion system with built in contour processing for multiple passive markers. And with a higher speed potential we have introduced a non-scanned sensor detection system for multiple active LED-markers, with improved ambient and background light rejection, obviating infrared markers and associated reflection problems.

With this kind of equipment, the methodological question of high-speed requirements for gait and other human motion studies should be settled in one laboratory having access to both device types. The investigations reported in (Winter, 1982) do not decide the case between 60 and 30 Hz television, or 50 and 25 Hz movie cameras, as the article states that the digitalized displacement coordinates were low-pass filtered with cut-off at 5 Hz. One would be intrigued to find great differences after further processing.

With the presented devices, we will in a collaborative clinical effort be in a position to analyse movement frequency components up to 100 Hz (or more with less LED's). These applications should contribute to decisive and hopefully indeed relaxed recommendations on sampling rate with opto-electronic or movie devices. Human movement studies would benefit from confidence that adequate speeds are provided by passive non-wired marker systems like movie or tv.

PRINCIPLE OF DIGITAL CONVERSION OF BRIGHT SPOT'S POSITION

VERTICAL COORDINATE Y CODED BY COUNTING AS LINE NUMBER
USEFUL RANGE 1 - 345 (9 BIT)

HORIZONTAL COORD. X CODED BY COUNTING TIME INCREMENTS ON 44 µs LINE SWEEP
USEFUL RANGE 1 - 455 (9 BIT)

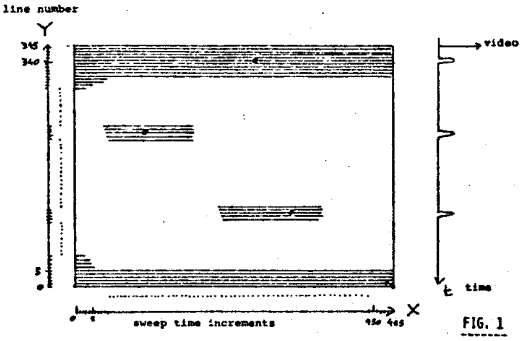

FIG. 1

MODE 2 3 A 3 B

FIG. 2

* CENTER OF GRAVITY OF MARKER
TO BE ESTIMATED FROM WHOLE CONTOUR, 4 OR 2 POINTS

INTELLIGENT VIDEO CONVERTER FIG. 3

REAL-TIME ESTIMATION OF EACH MARKER'S CENTRE-OF-GRAVITY BY BUILT-IN MICROPROCESSOR FOR FURTHER DATA REDUCTION

1. PER MARKER j PER LINE n
   FAST ADD/SUBTRACT/MULTIPLY HARDWARE CALCULATES:

   $S_{X_{jn}} = X_{jn2} + X_{jn1}$ $\qquad D_{X_{jn}} = X_{jn2} - X_{jn1}$

   $P_{X_{jn}} = 1/2\ S_{X_{jn}}.D_{X_{jn}}$ $\qquad P_{Y_{jn}} = Y_{jn}.D_{X_{jn}}$

2. PER TV-FRAME, ALL MARKERS, THESE NUMBERS ARE BUFFERED AND TRANSFERRED TO MICROPROCESSOR MEMORY

3. PER TV-FRAME, MICROPROCESSOR COLLECTS PREVIOUS NUMBERS, PER MARKER j, ALL RELEVANT n, AND CALCULATES CENTRE-OF-GRAVITY ESTIMATES:

$$X_{c_j} = \frac{\sum_n P_{X_{jn}}}{\sum_n D_{X_{jn}}} \qquad Y_{c_j} = \frac{\sum_n P_{Y_{jn}}}{\sum_n D_{X_{jn}}}$$

4. OUTPUT TO POST-PROCESSOR IS FOR EACH MARKER j JUST ONE COORDINATE-PAIR (X_{c_j}, Y_{c_j})

FIG. 4

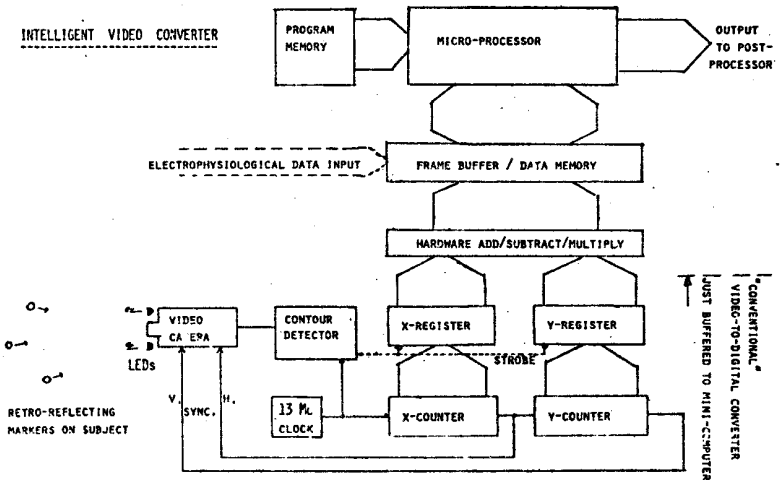

POSITION-SENSITIVE DEVICE (PSD) IS NON - SCANNED SENSOR
WITH 4 ACTIVE ELECTRODES & 1 RETURN

LIGHT SPOT POSITION EXTRACTED FROM 4 PARTIAL - CURRENT VALUES:

$$X_{LED} :: \frac{I_x - I'_x}{I_x + I'_x} \qquad Y_{LED} :: \frac{I_y - I'_y}{I_y + I'_y}$$

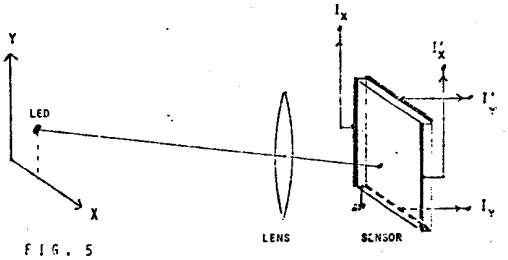

FIG. 5

SYNCHRONOUS DETECTOR PRINCIPLE

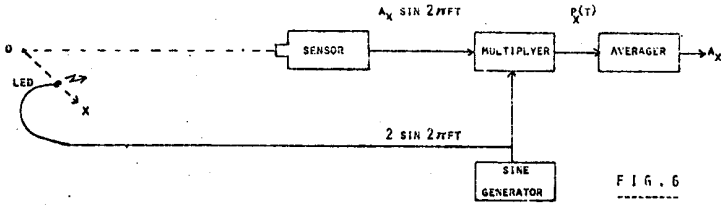

FIG. 6

BLOCK DIAGRAM
SYNCHRONOUS DETECTOR
MULTIPLE-LED SYSTEM

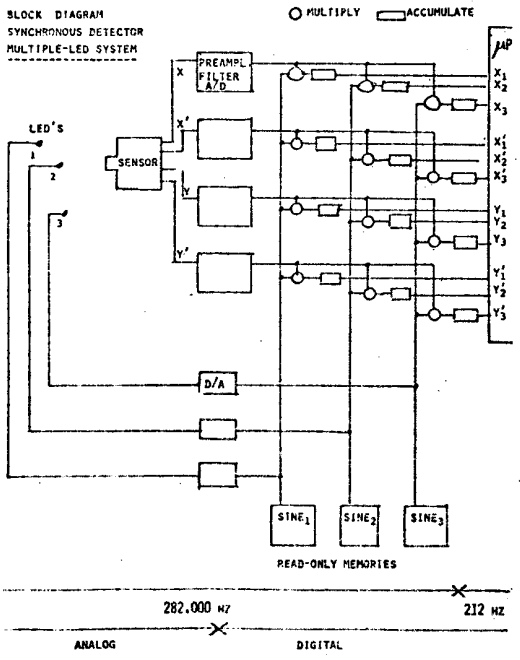

FIG. 7

FIG. 8

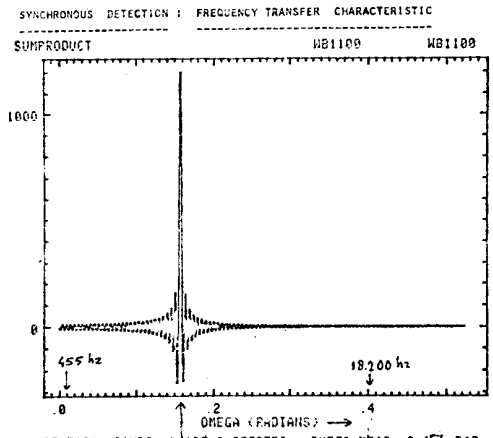

$M_R = 238$ hz; $F_{MEAS} = 7.143$ hz. $\tau_{SAMPLE} = 3.5\,\mu s$

FIG. 9

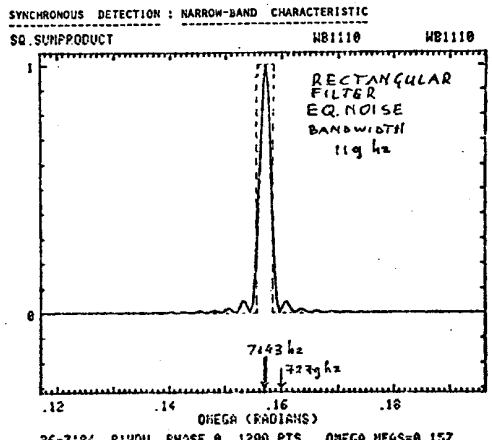

$M_R = 238$ /s $\tau_{SAMPLE} = 3.5\,\mu s$

REFERENCES

1. Cappozzo, A. (1983), Considerations on clinical gait evaluation. J. Biomechanics, Vol. 15 p. 302.

2. Dinn, D.F., and Winter, D.A. (1970) CINTEL, computer interface for television. IEEE Trans. on Computers, nov. 1970, pp 1091-1095.

3. Furnee, E.H. (1967), Hybrid instrumentation in prosthetics research. In: Digest 7th Int. Conf. on Medical and Biological Engineering, Stockholm.

4. Harris, F.J. (1978), On the use of windows for harmonic analysis with the discrete Fourier transform. Proc. IEEE, Vol. 66. no.1, pp. 51-83.

5. Jarrett, M.O., Andrews, B.A. and Paul, J.P. (1974), Quantitative analysis of locmotion using television, 1974 World Congress of ISPO, INTERBOR & APO, Montreux.

6. Jarrett, M.O. (1976) A television/computer system for human locomotor analysis. Doct. Thesis june 1976, University of Strathclyde, Glasgow.

7. Lindholm, L.E. and Oeberg, K.E.T. (1974) An opto-electronic instrument for remote on-line movement monitoring. Biotelemetry 1 pp 94-95.

8. SELSPOT, trade literature, SELCOM AB, Partille, Sweden.

9. Taylor, K.D. e.a. (1982) An automated motionmeasurement system for clinical gait analysis, J. Biomechanics Vol. 15, no 7, pp. 505 - 516 .

10. Waas, R.C. (1969) A digital optical scanning system for kinematic analysis. Ph.D. Thesis, Case Western Reserve University, Cleveland.

11. Wallmark, J.T. (1957) A new semiconductor photocell using lateral photoeffect. Proc. IRE 45 pp 474-483.

12. Whittle, M.W. (1982) Calibration and performance of a 3-dimensional television system for kinematic analysis. J. Biomechanics Vol. 15 no. 3, pp 185-196.

13. Winter, D.A. (1982) Camera speeds for normal and pathological gait analyses. J. Medical Engineering and Computing, Vol. 20, pp. 408-412.

14. Woltring, H.J. (1975) Calibration and measurement in 3-dimensional monitoring of human motion by optoelectronic means. Biotelemetry 2, pp 169-196.

15. Woltring, H.J. (1980), Planar control in multi-camera calibration for 3-D gait studies. J. Biomechanics Vol. 13, pp 39-48.